Article

Fast-moving stars around an intermediatemass black hole in ω Centauri

https://doi.org/10.1038/s41586-024-07511-z

Received: 15 December 2023

Accepted: 2 May 2024

Published online: 10 July 2024

Open access



Check for updates

Maximilian Häberle^{1⊠}, Nadine Neumayer¹, Anil Seth², Andrea Bellini³, Mattia Libralato^{4,5}, Holger Baumgardt⁶, Matthew Whitaker², Antoine Dumont¹, Mayte Alfaro-Cuello⁷, Jay Anderson³, Callie Clontz^{1,2}, Nikolay Kacharov⁸, Sebastian Kamann⁹, Anja Feldmeier-Krause^{1,10}, Antonino Milone¹¹, Maria Selina Nitschai¹, Renuka Pechetti⁹ & Glenn van de Ven¹⁰

Black holes have been found over a wide range of masses, from stellar remnants with masses of 5–150 solar masses (M_{\odot}) , to those found at the centres of galaxies with $M > 10^5 M_{\odot}$. However, only a few debated candidate black holes exist between 150 M_{\odot} and 10⁵M_o. Determining the population of these intermediate-mass black holes is an important step towards understanding supermassive black hole formation in the early universe^{1,2}. Several studies have claimed the detection of a central black hole in ω Centauri, the most massive globular cluster of the Milky Way³⁻⁵. However, these studies have been questioned because of the possible mass contribution of stellar mass black holes, their sensitivity to the cluster centre and the lack of fast-moving stars above the escape velocity⁶⁻⁹. Here we report the observations of seven fastmoving stars in the central 3 arcsec (0.08 pc) of ω Centauri. The velocities of the fastmoving stars are significantly higher than the expected central escape velocity of the star cluster, so their presence can be explained only by being bound to a massive black hole. From the velocities alone, we can infer a firm lower limit of the black hole mass of about 8,200M_o, making this a good case for an intermediate-mass black hole in the local universe.







Stellar Mass BHs



Comparison of several stellar black holes in our galaxy



This artist's impression compares side-by-side three stellar black holes in our galaxy: Gaia BH1, Cygnus X-1 and Gaia BH3, whose masses are 10, 21 and 33 times that of the Sun respectively. Gaia BH3 is the most massive stellar black hole found to date in the Milky Way. The radii of the black holes are directly proportional to their masses, but note that the black holes themselves have not been directly imaged.

Credit: ESO/M. Kornmesser



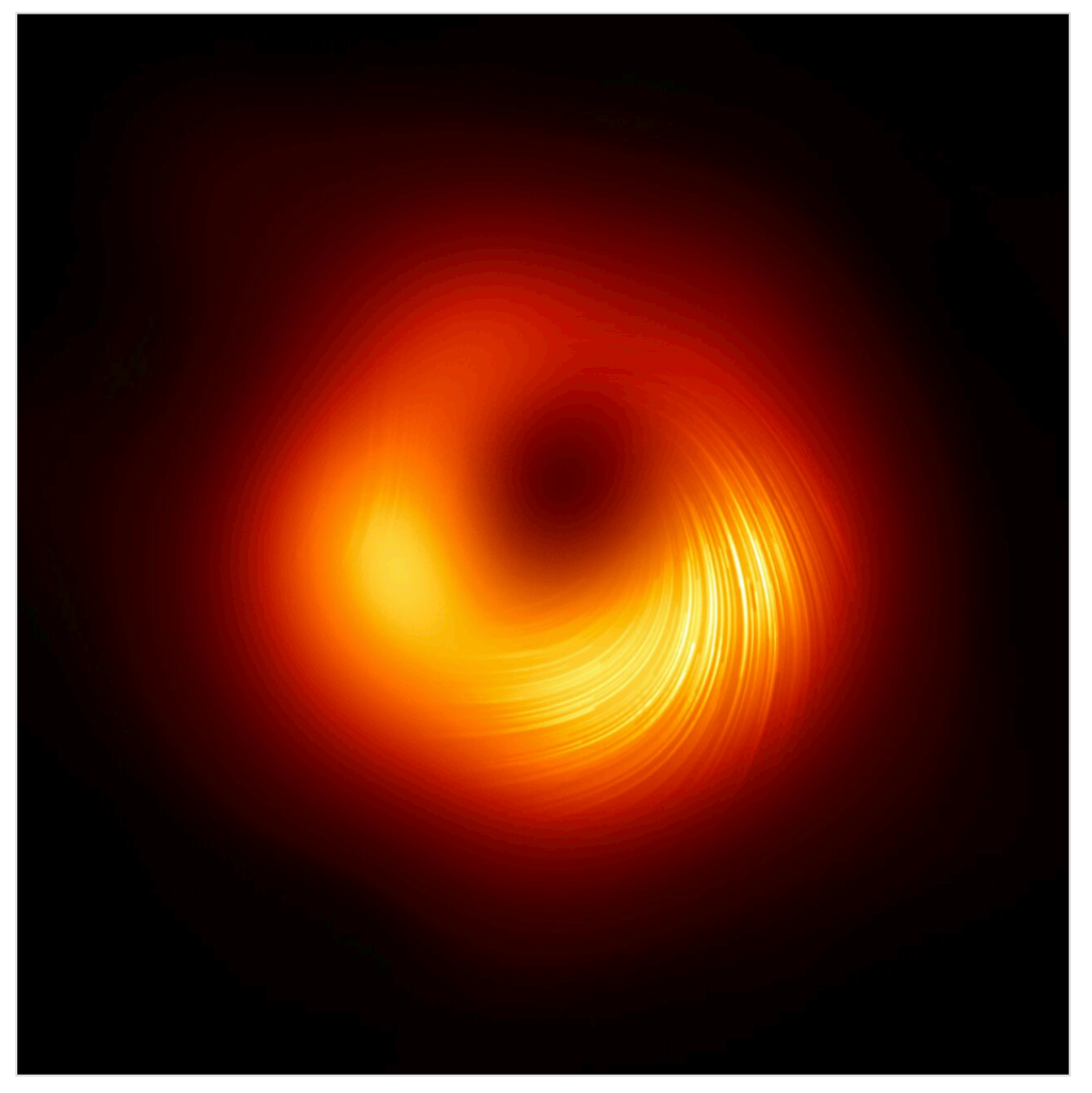




Super Massive BHs



A view of the M87 supermassive black hole in polarised light



The Event Horizon Telescope (EHT) collaboration, who produced the first ever image of a black hole released in 2019, has today a new view of the massive object at the centre of the Messier 87 (M87) galaxy: how it looks in polarised light. This is the first time astronomers have been able to measure polarisation, a signature of magnetic fields, this close to the edge of a black hole.

This image shows the polarised view of the black hole in M87. The lines mark the orientation of polarisation, which is related to the magnetic field around the shadow of the black hole.

Credit: EHT Collaboration







IMBHs

Intermediate mass black holes (IMBHs) are an elusive class of black holes that are expected to lie in the ~10² : ~10⁵ M_☉ range, between the stellar-mass black holes and 10⁶ M_☉ supermassive black holes.

Their existence is theorized, and evidence suggests they may form in dense star clusters. Evidence suggests IMBHs may reside in the cores of some globular clusters, inferred from the motions of stars within them.

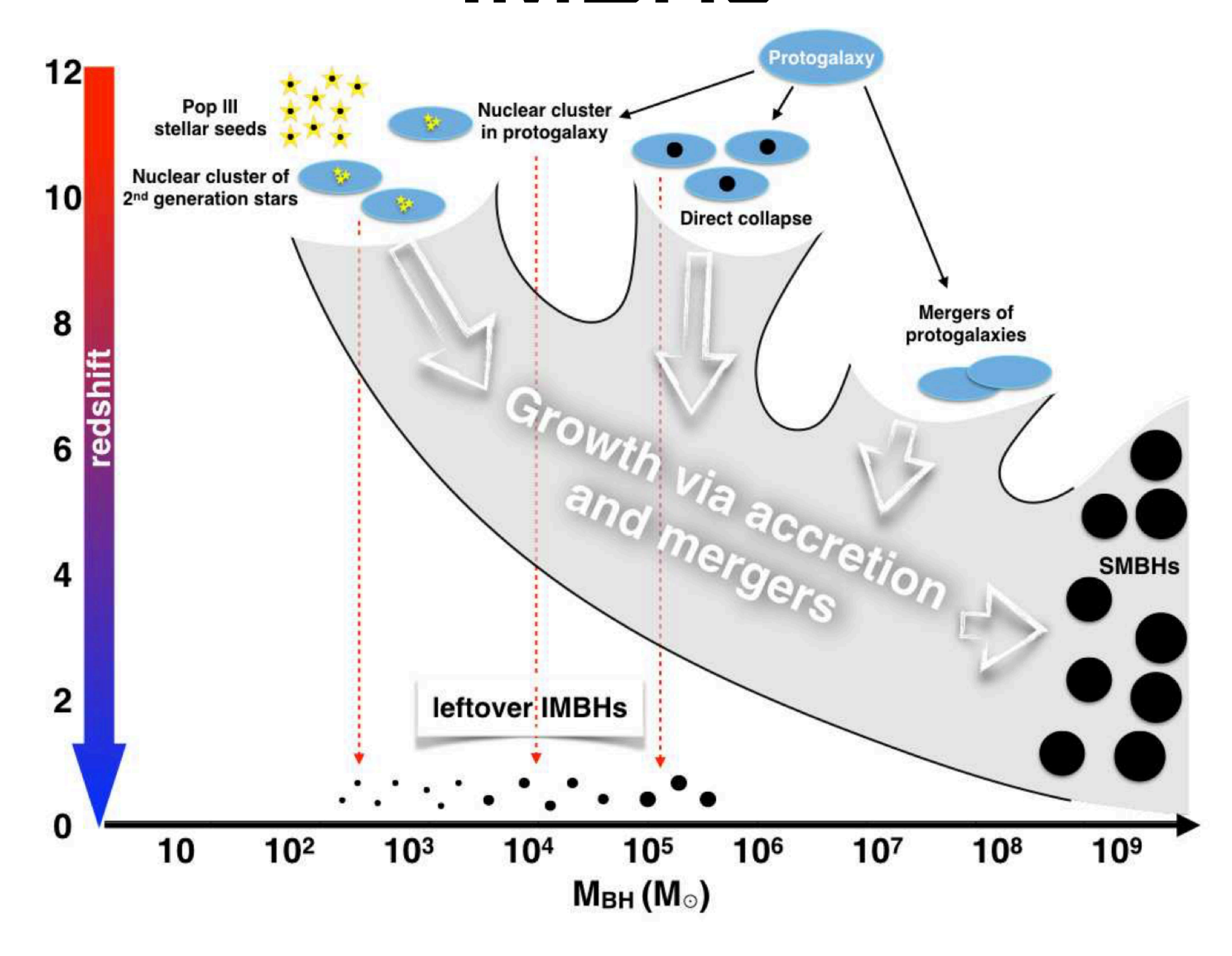
The wealth of observational confirmations for the existence of smaller mass BHs (~200 M_☉) and SMBHs stands in stark contrast to the scarcity of observational evidence in favor of the existence of BHs between these two mass regimes.

Koliopanos 2017





IMBHs



Koliopanos 2017





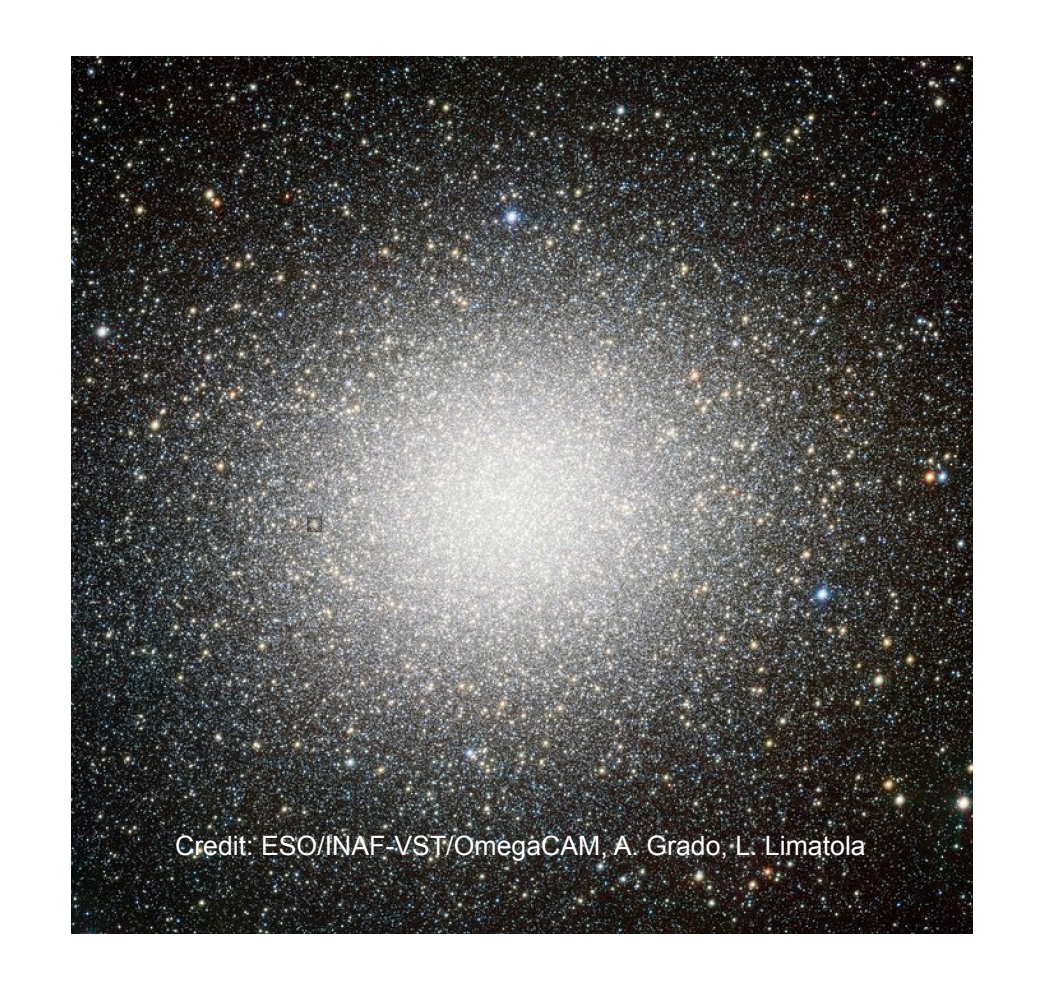


The case of ω Centauri

Omega Centauri (ω Cen - NGC5139) is the brightest Globular Cluster (GC) visible in the sky and also the largest orbiting the Milky Way

- Mass ~ 3.94 · 10⁶ M_☉
- Distance ~ 5430 pc
- V-band magnitude ~ 3.50

Baumgardt et al. 2018

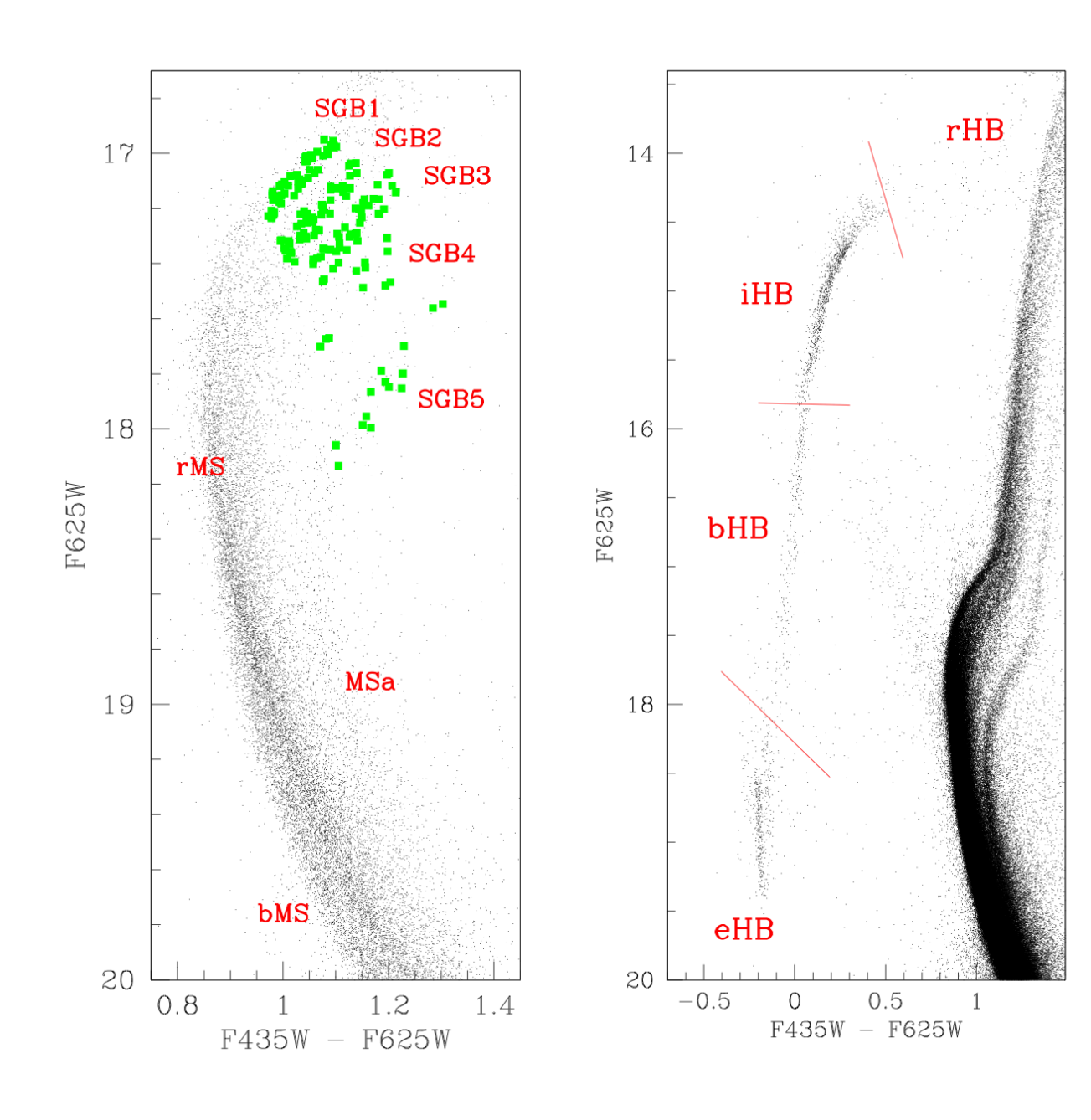






The case of ω Centauri

- spread in age (?)
- spread in metallicity
- complex chemical composition



Tailo et al. 2016

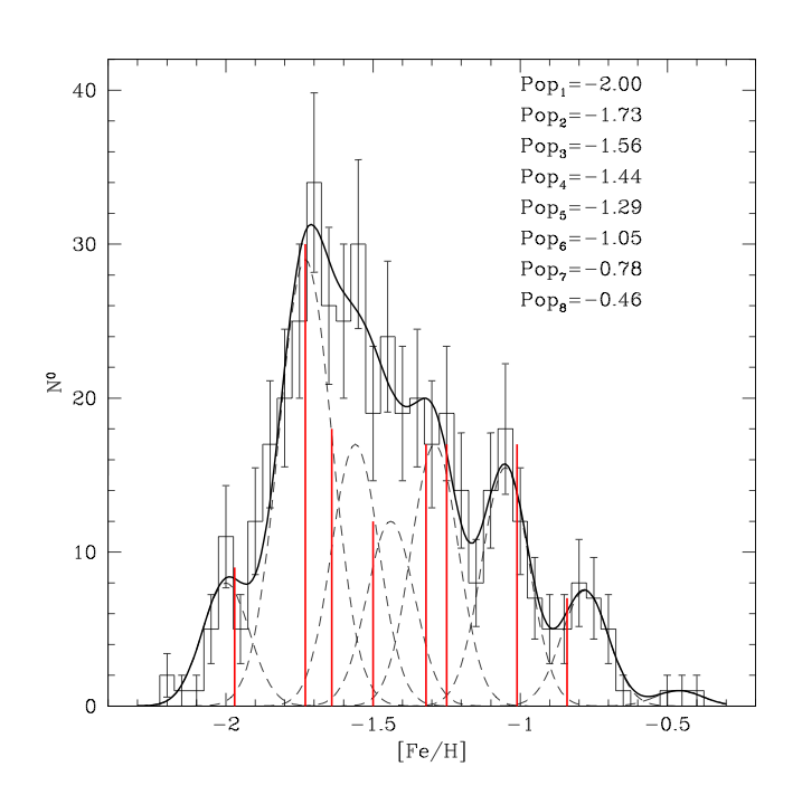




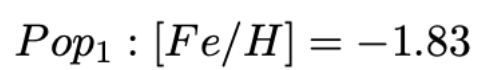


The case of ω Centauri

- spread in age (?)
- spread in metallicity
- complex chemical composition



Villanova et al. 2014



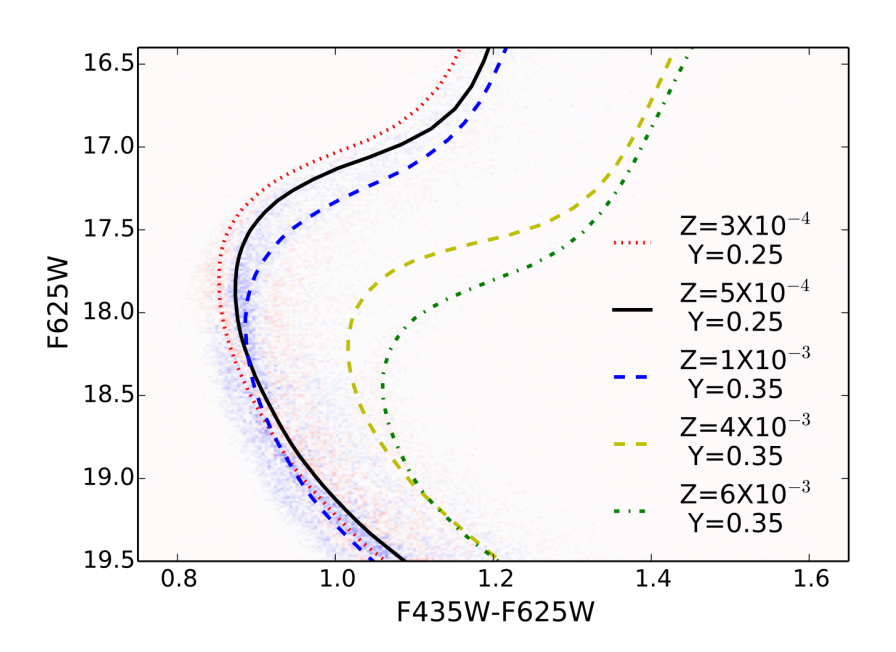
$$Pop_2 : [Fe/H] = -1.65$$

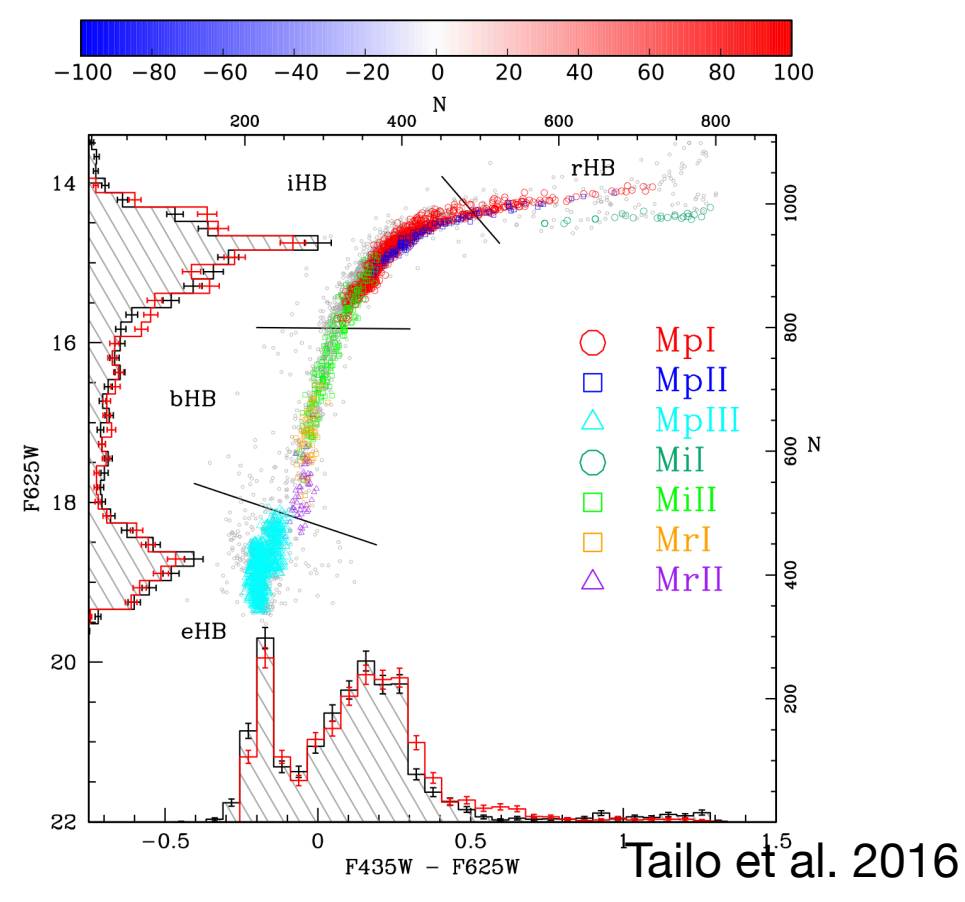
$$Pop_3 : [Fe/H] = -1.34$$

$$Pop_4: [Fe/H] = -1.05$$

$$Pop_5 : [Fe/H] = -0.78$$

$$Pop_6: [Fe/H] = -0.42$$







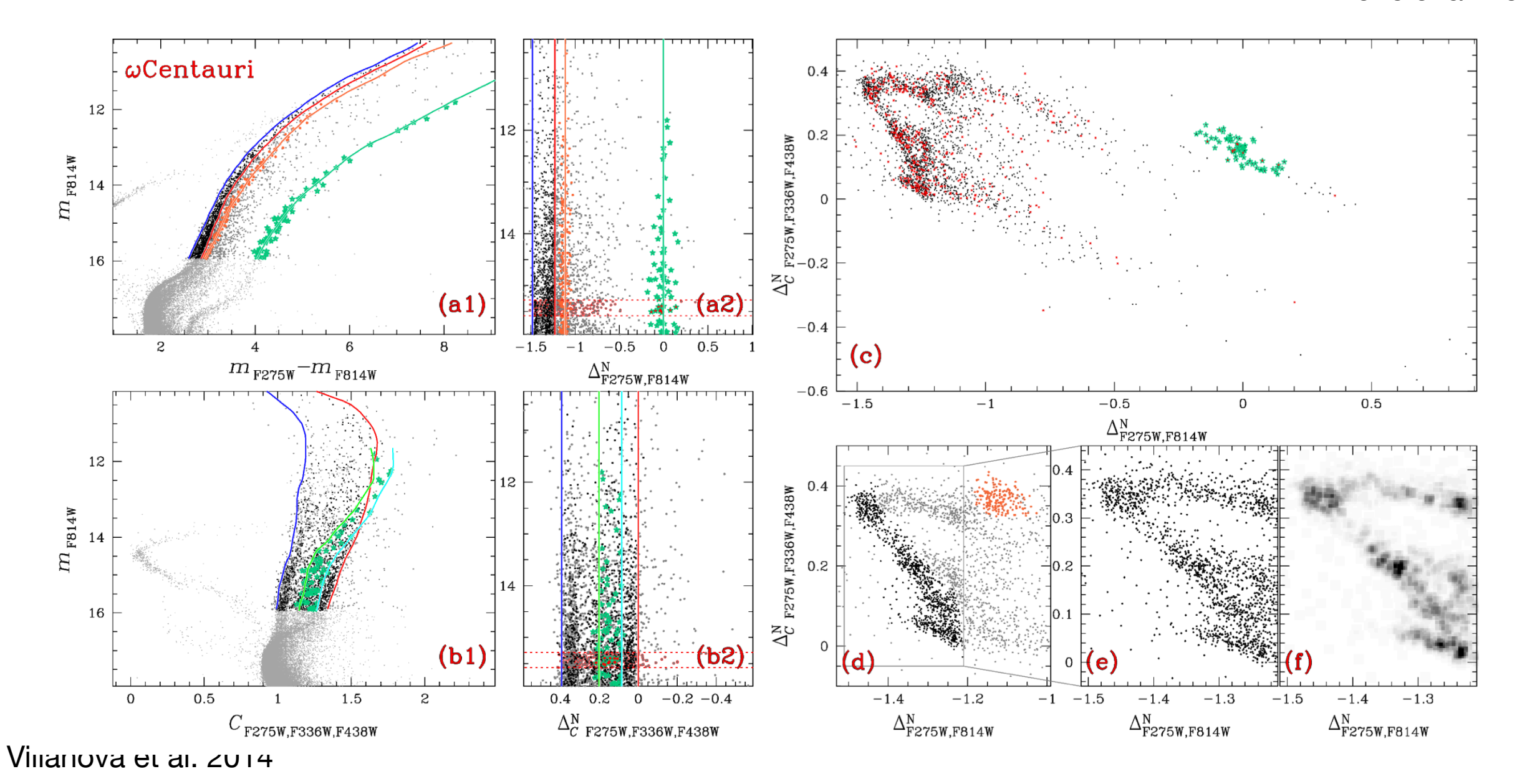




The case of ω Centauri

complex chemical composition

Milone et al. 2017









The case of ω Centauri

The observed wide spread in chemical composition suggests it had enough mass and gravity to retain gas and continue forming stars over billions of years, as a small galaxy would do.

Hilker & Richer 2000

Its orbit around the Milky Way is **strongly retrograde** (moving in the opposite direction of the Galactic rotation), which is unusual for most globular clusters but consistent with a large object captured from outside the Milky Way's disk (Gaia-Sausage-Enceladus stripped nucleus?)





Data

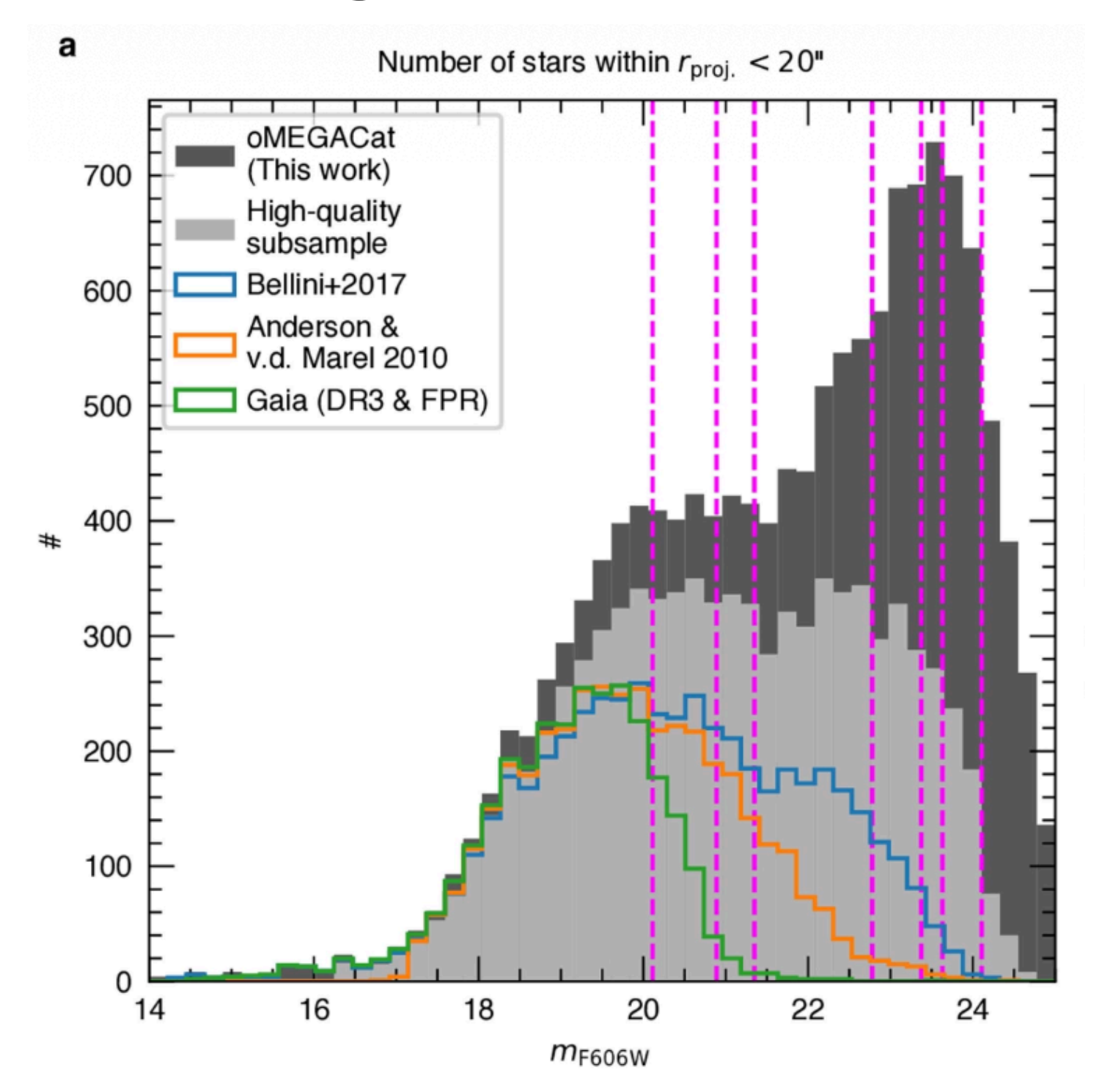
- 500 Hubble Space Telescope archival images take over a time span of 20 years. The unprecedented depth and precision of this catalogue have enabled us to discover a statistically significant overdensity of fast-moving stars in the centre of the cluster
- Used the state-of-the-art photometry tool KS2 for the source detection and the astro-photometric measurements
- Proper-motion catalogue with high-precision measurements for 1.4 million stars out to the half-light radius
 of ω Cen
- Owing to the large number of observations, some stars in the central region have up to 467 individual
 astrometric measurements the catalogue reaches unprecedented depth
- Cuts on the quality of the proper-motion fit required both a proper-motion error less than 0.194 mas/yr ≈ 5 km/s and a reduced χ2 < 10 for the linear proper-motion fit for both the RA and Dec measurements. Apart from these quality selections, we also required the star to lie on the CMD sequence in an HST-based CMD
- The highest precision is achieved in the well-covered centre of the cluster, in which our proper motions have a median error of only about 6.6 µas/yr (0.17 km/s) per component for bright stars.







Catalog completeness

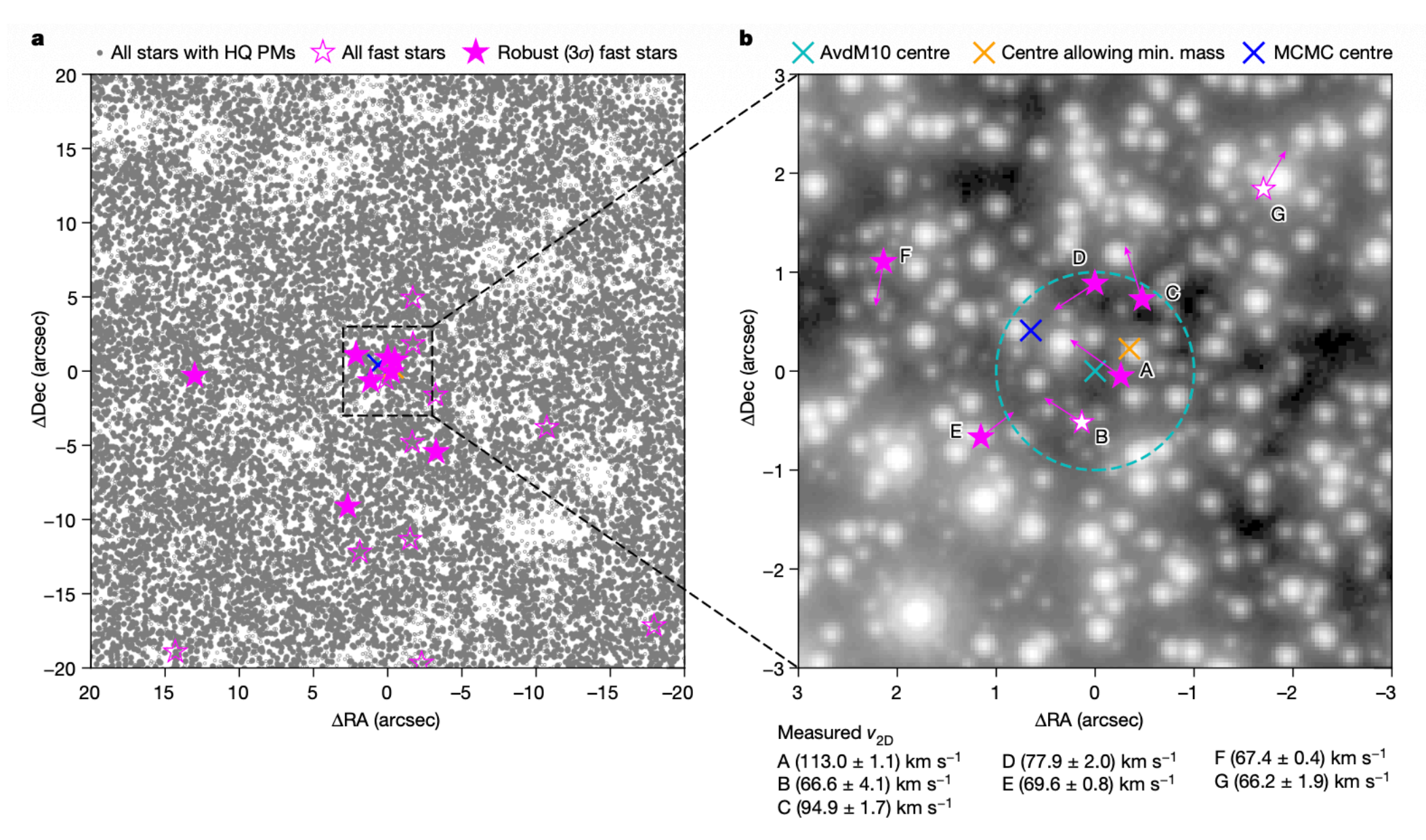








Spatial location of fast moving stars



Solid grey markers indicate all stars with a high-quality proper motion measurement in our new catalogue within a $40'' \times 40''$ region centered on the AvdM10 centre. Well-measured stars with velocities higher than the cluster escape velocity (62 km s-1) and lying on the cluster main sequence in the colour-magnitude diagram (Fig. 2) are marked in pink. We use filled markers for stars that are at least 3σ above the escape velocity, and open markers for all other stars above the escape velocity.







Location of fast moving stars in the CMD

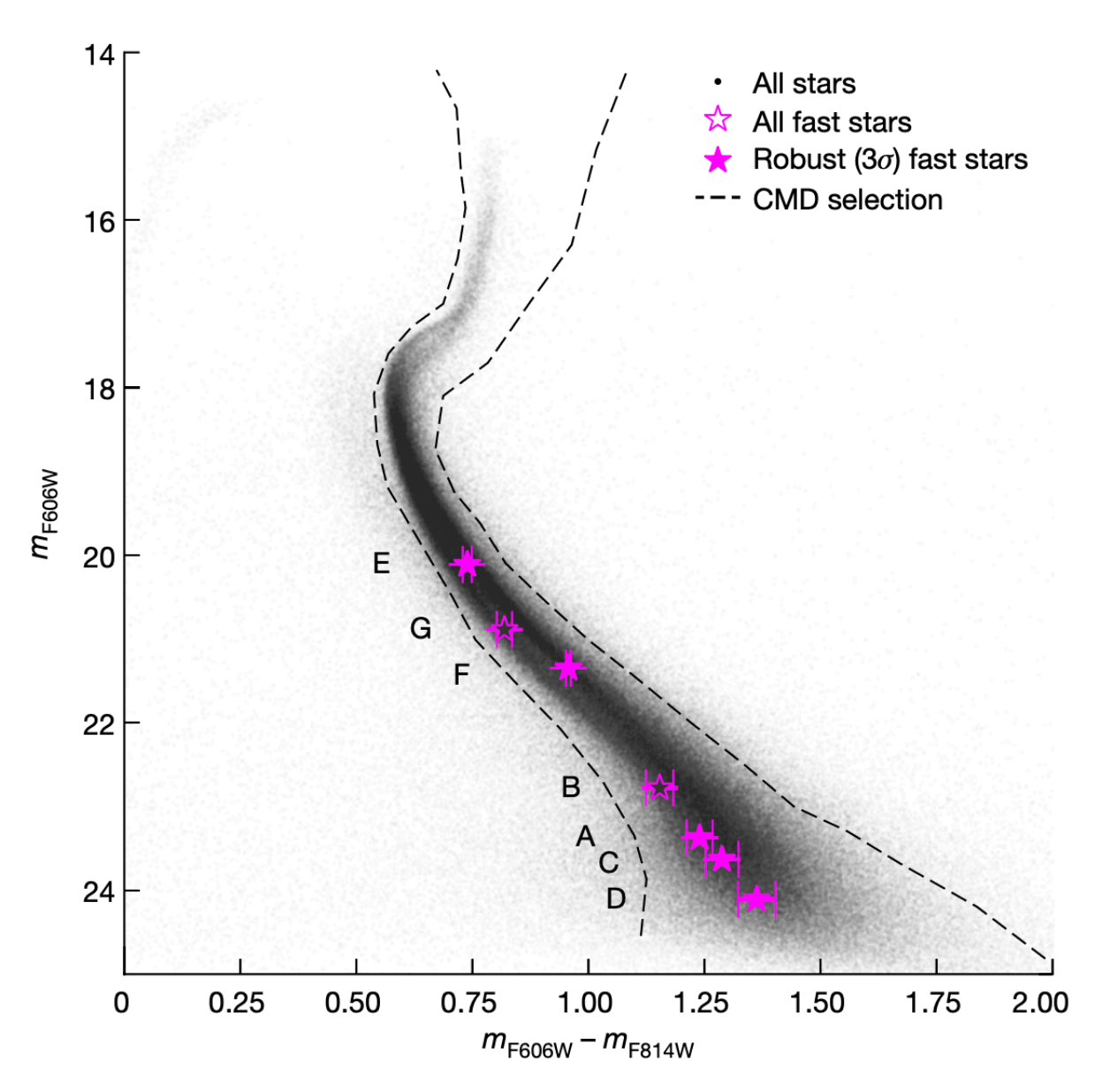


Fig. 2 | HST-based colour-magnitude diagram (CMD) of ω Cen. The CMD locations of all fast-moving stars are marked with pink symbols, with their photometric 1σ errors marked with error bars. All of them lie on the main sequence, showing that they are probably members of ω Cen. The stars are labelled from A to G, sorted by their distance from the AvdM10 centre.







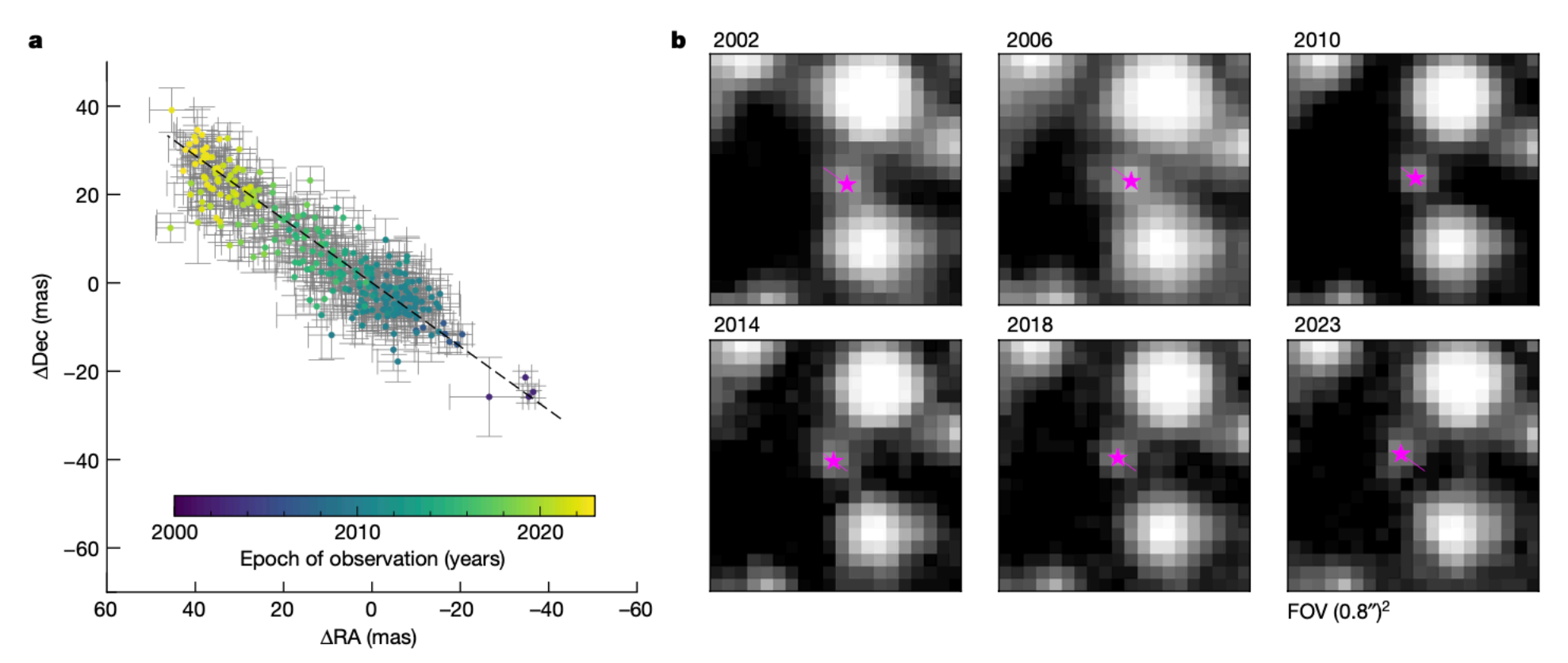


Fig. 3 | **Motion of the fastest star. a**, Individual measured positions with 1σ error bars. **b**, Multi-epoch HST imaging for star A, the fastest ($v_{\text{projected}} = 113.0 \pm 1.1 \, \text{km s}^{-1}$) and centremost of the seven fast-moving stars discovered in the centre of ω Cen. The star is indicated with a pink marker on the images and

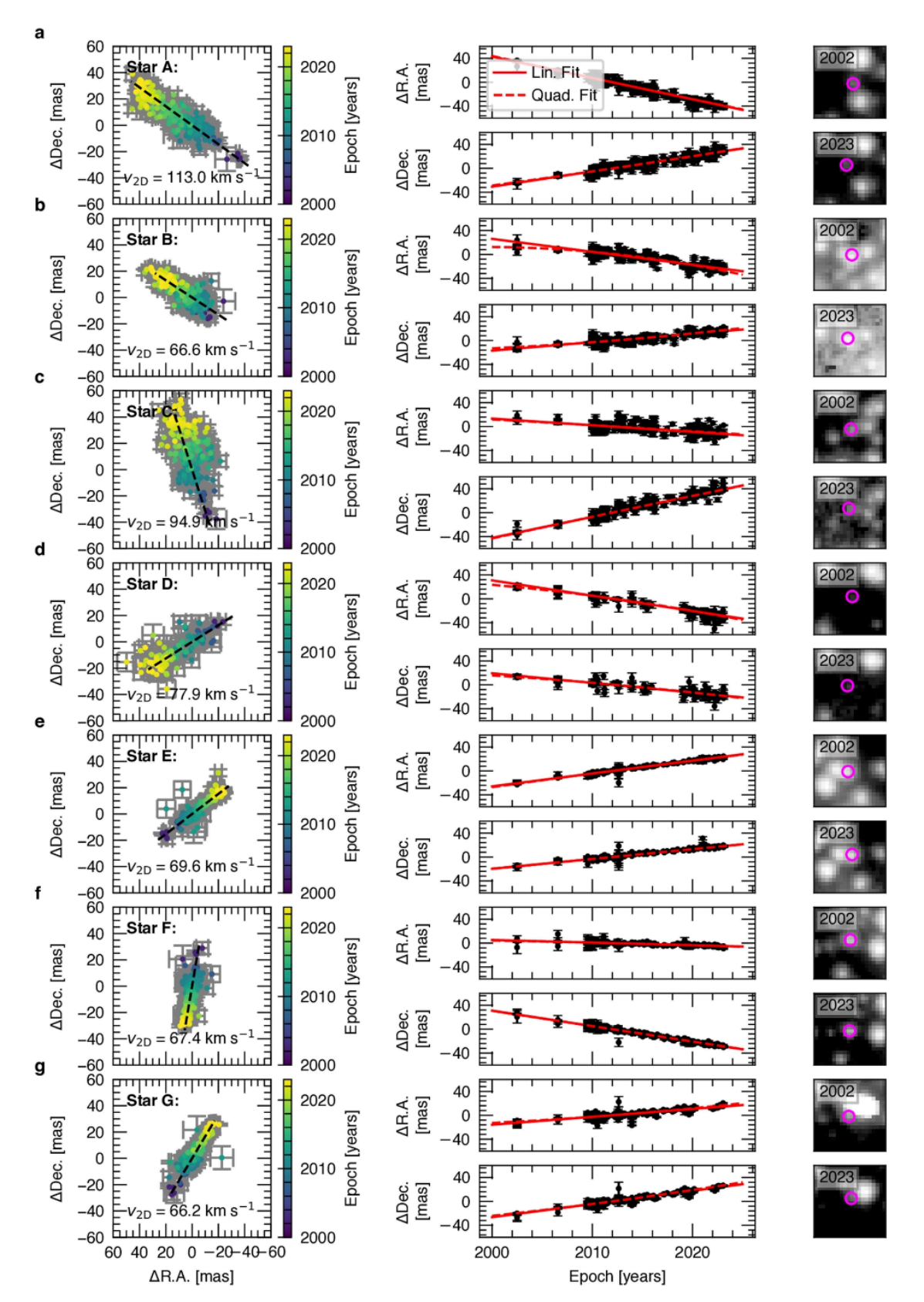
its motion over 21 years with a line. This plot shows the notable astrometric quality and the long temporal baseline we have in our unique dataset. Similar plots for all other stars are shown in Extended Data Fig. 2. Dec, declination; RA, right ascension; FOV, field of view.

The presence of the seven central stars moving faster than the escape velocity of the cluster can be explained only if they are bound to a compact massive object near the centre, raising the local escape velocity. If no massive object was present, their velocities would cause them to leave the central region in less than 1,000 years, and then eventually escape the cluster. These fast-moving stars are a predicted consequence of an IMBH, but these stars are not expected from mass-segregated stellar-mass black holes









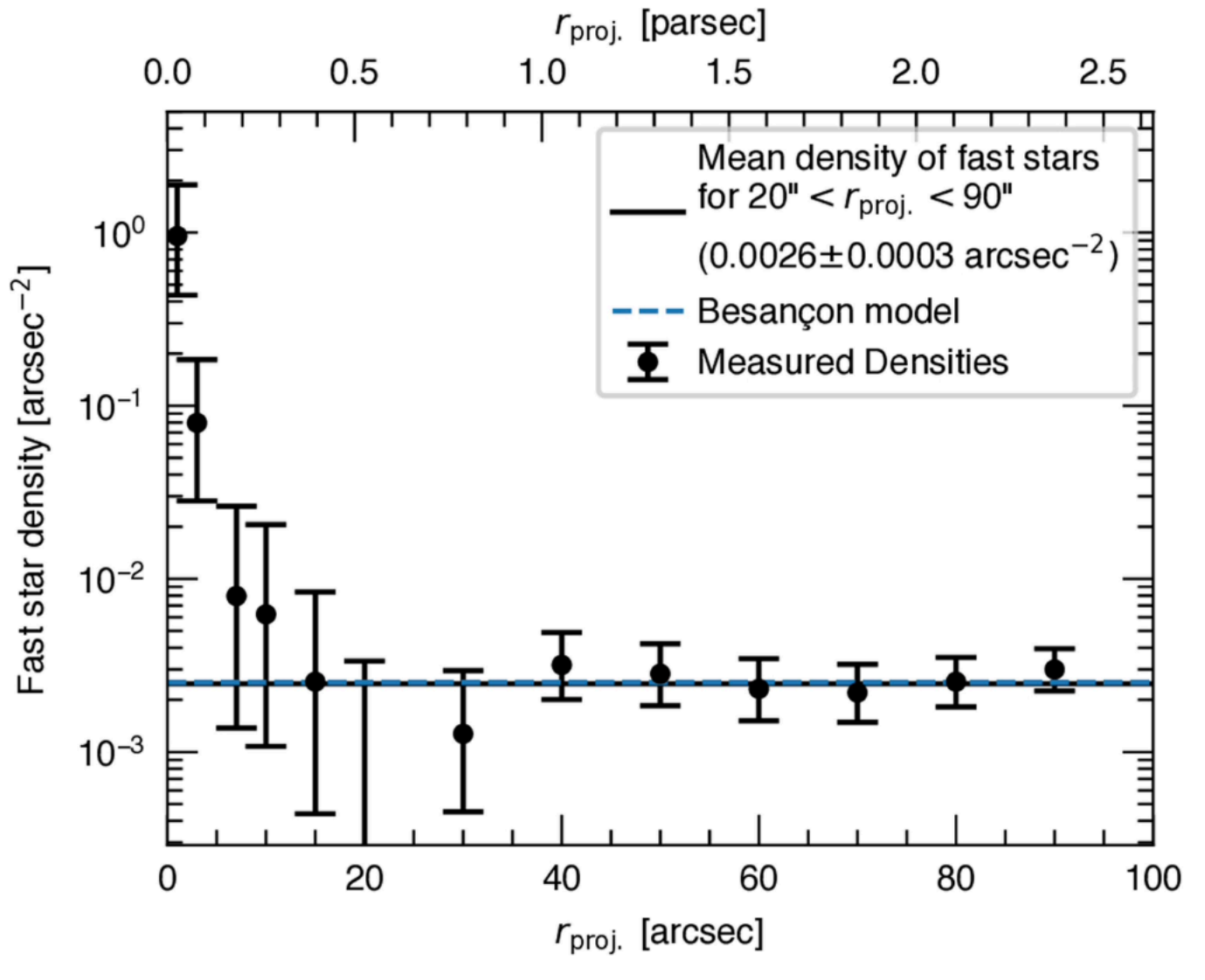
Extended Data Fig. 2 | Astrometry and multi epoch imaging for all fastmoving stars. Each row (a-g) shows the astrometry and imaging for one of the seven fast-moving stars. The left column shows the raw astrometric measurements used to determine the proper motions, colour-coded by the $epoch\ of\ their\ observation.\ The\ centre\ column\ shows\ the\ linear\ and\ quadratic$

 $fits \, to \, both \, the \, R.A. \, and \, Dec. \, position \, change \, of \, the \, stars. \, Error bars \, correspond$ to the 1σ error on the individual position measurements. The right column shows stacked images from 2002 (ACS/WFC F625W) and 2023 (WFC3/UVIS F606W); the positions of the fast stars are marked with a pink open circle.









Extended Data Fig. 1 | **Number density of fast-moving stars.** The black markers with errorbars (1σ ; based on Poisson statistics) show the measured number density of robustly detected fast-moving stars determined in radial bins with respect to ω Cen's center. A constant density of Galactic fore-/ background stars is expected, but we see a strong and statistically significant

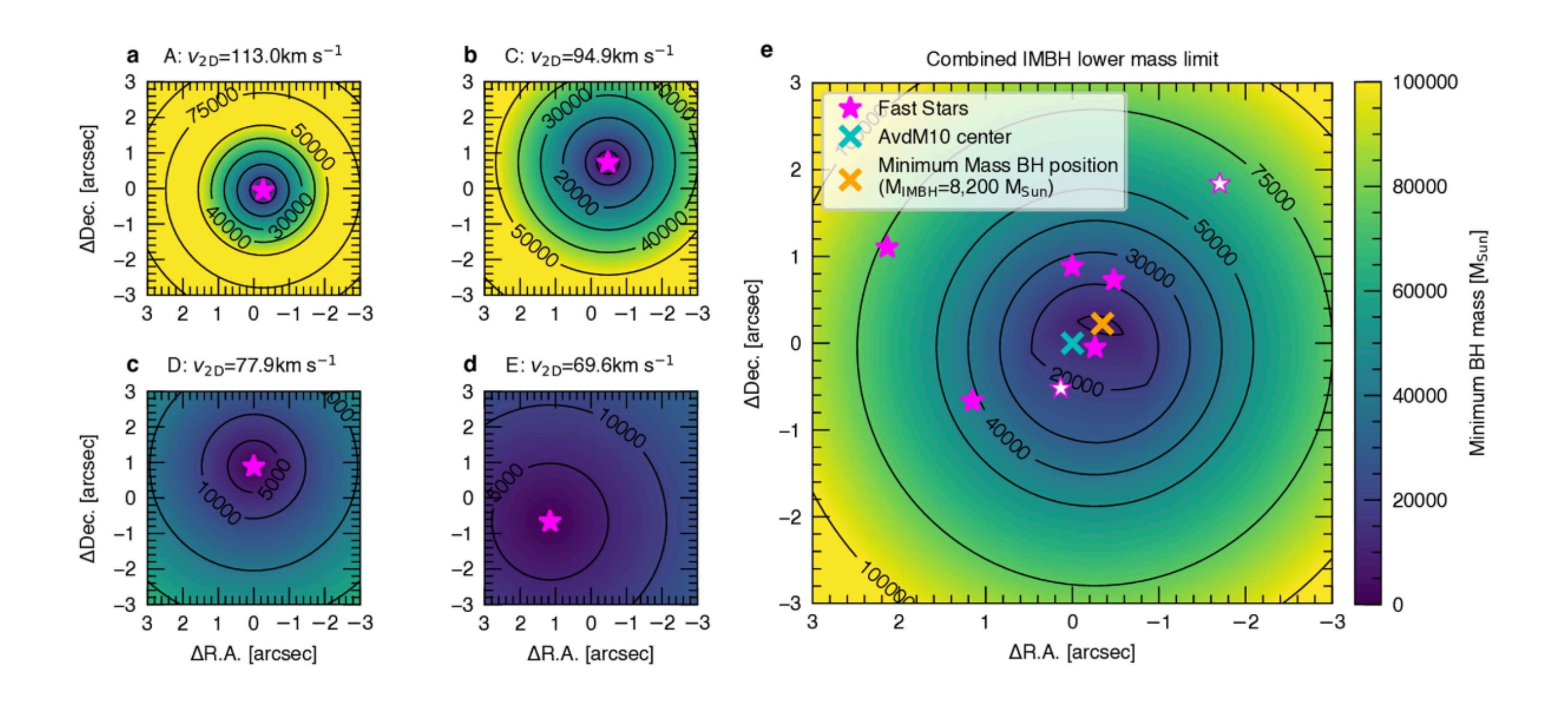
rise of the density towards the AvdM10 6 centre. Based on the number density of fast-moving stars at large radii (which is consistent with predictions from a Besançon Milky Way model, dashed line), only $\sim\!0.073$ fast-moving stars are expected within the central 3'' compared to the 5 observed stars.







Constraint of central black hole mass from escape velocity



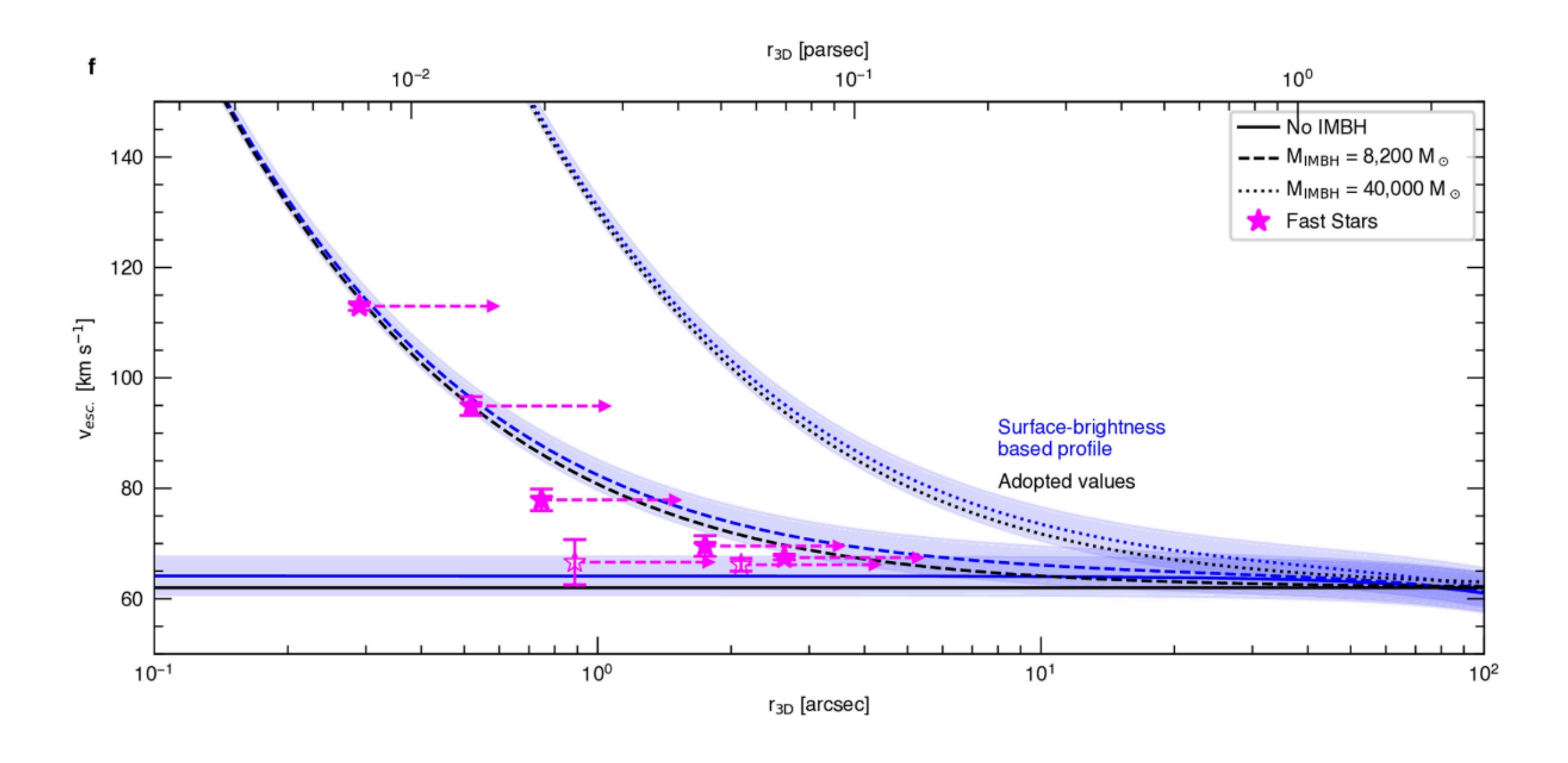
The presence of stars with velocities above the escape velocity of the cluster indicates that they are bound to a massive object. Since neither the mass nor the exact position of this object is known, only a lower mass limit for each possible 2D location can be inferred. The four left plots (a–d) show the contours of the minimum black hole mass indicated by the four centermost robustly measured fast-moving stars. By combining the minimum black hole mass constraints from each of the fast-moving stars, we can find the position that allows for the lowest IMBH mass (e). This analysis indicates a firm lower limit of around 8,200 M $_{\odot}$







Constraint of central black hole mass from escape velocity



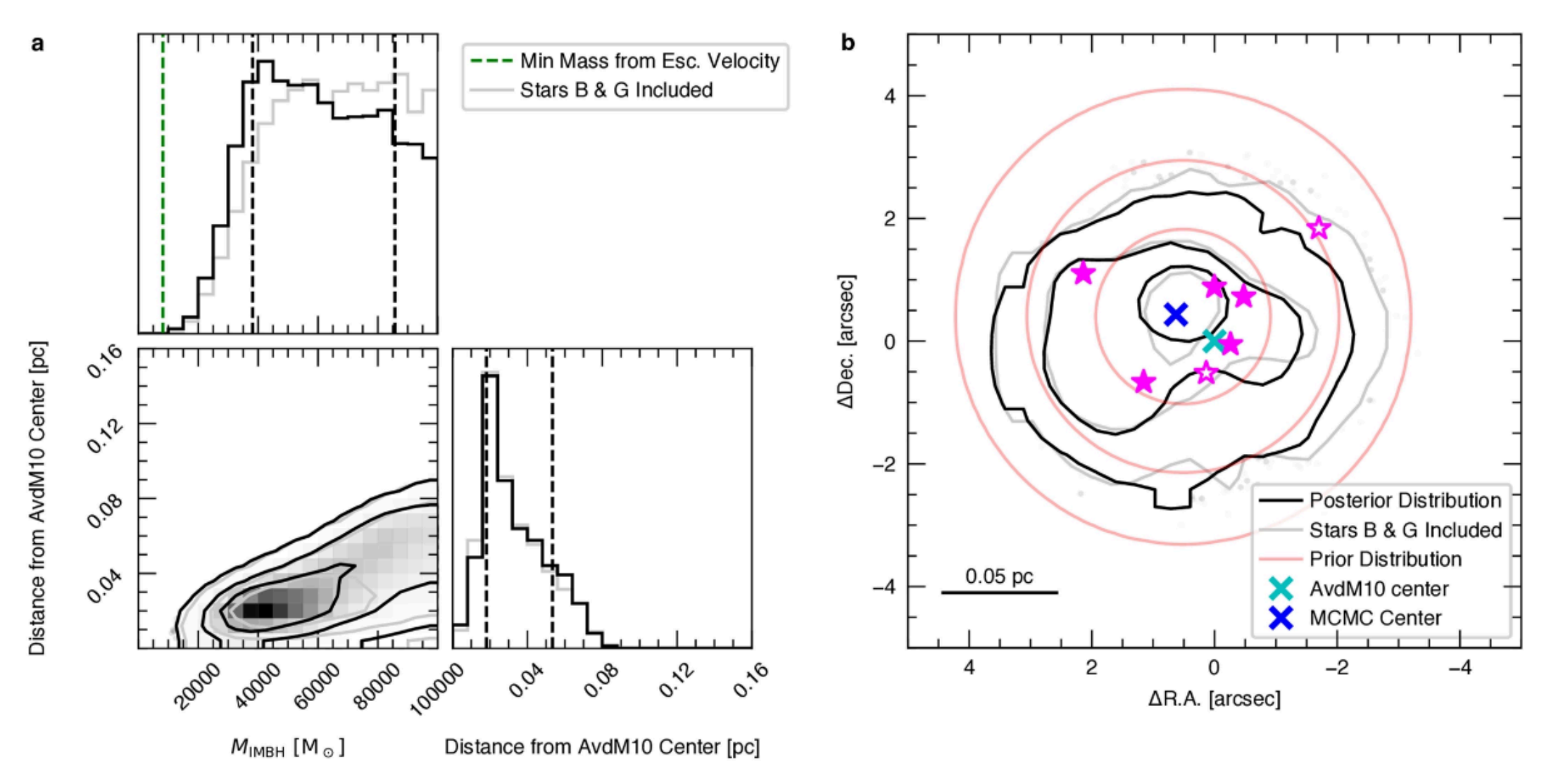
Results for a surface brightness profile based escape velocity profile in blue, using the surface brightness profile and the dynamical distance (5.43 kpc) and M/L ratio derived from N-body models, either without any IMBH, with a 8,200 M_{sun} IMBH, or a 40,000 M_{sun} IMBH. The radii are measured with respect to the minimum mass centre shown in e. The shaded regions indicate the uncertainty introduced by an assumed error of \pm 0.2 kpc on the distance. The surface-brightness profile based escape velocity is compatible with the adopted value of v_{esc} = 62 km/s. The profile without an IMBH is also nearly flat in the inner ~50″, justifying the assumption of a flat profile in the innermost region.







Constraint of central black hole mass from acceleration



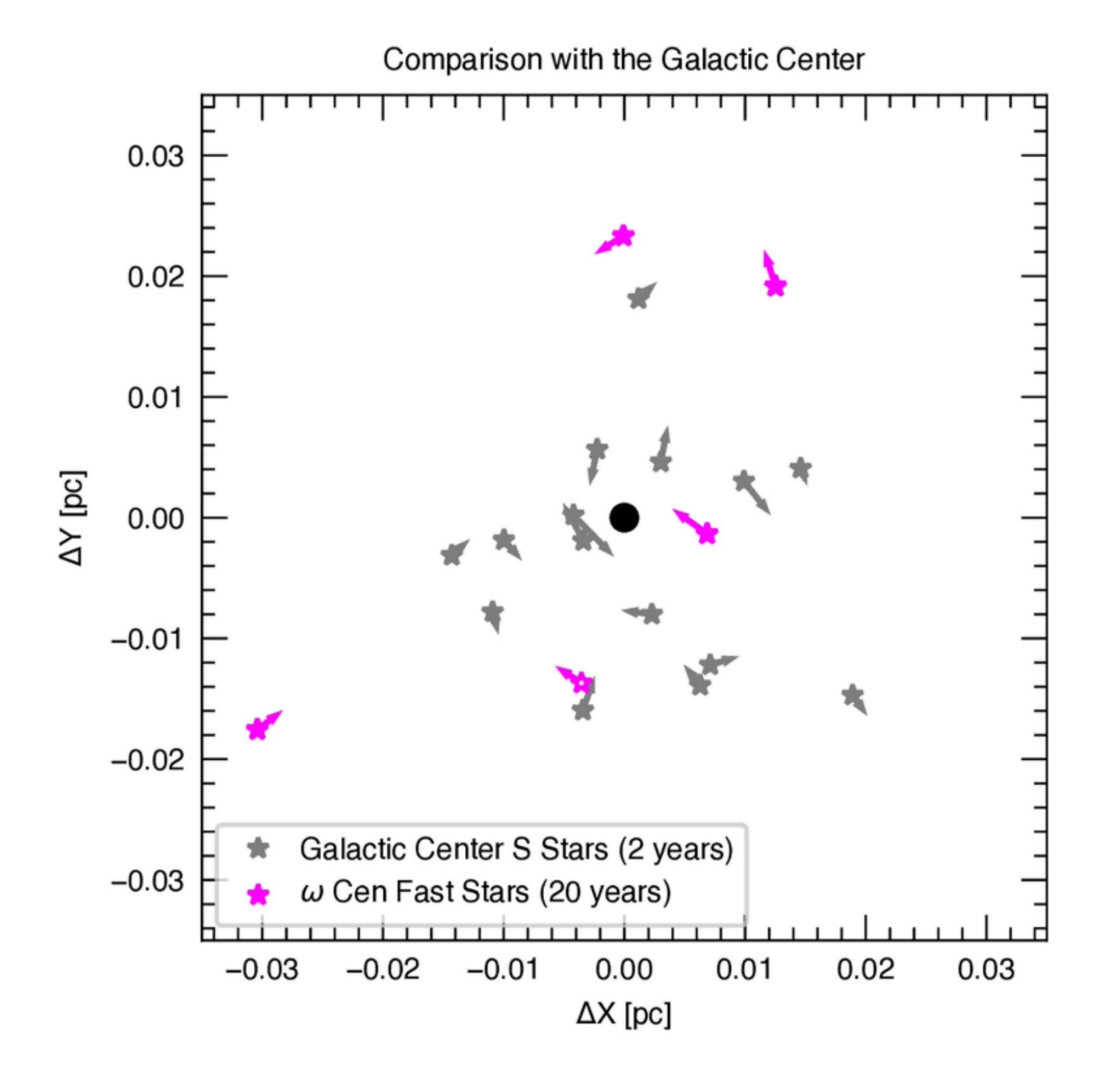
Extended Data Fig. 6 | Constraints on the IMBH using the acceleration measurements. Taking into account the limits on the accelerations gives us additional constraints on black hole mass (a) and on-sky position (b). The contours shown correspond to the 1-, 2-, and 3-sigma levels of the distribution.

This analysis using both escape velocity and acceleration measurements from the five robustly measured fast stars constrains the minimum IMBH mass stronger than escape velocity constraints alone. Both plots also show the distribution from an MCMC run including stars B and G.







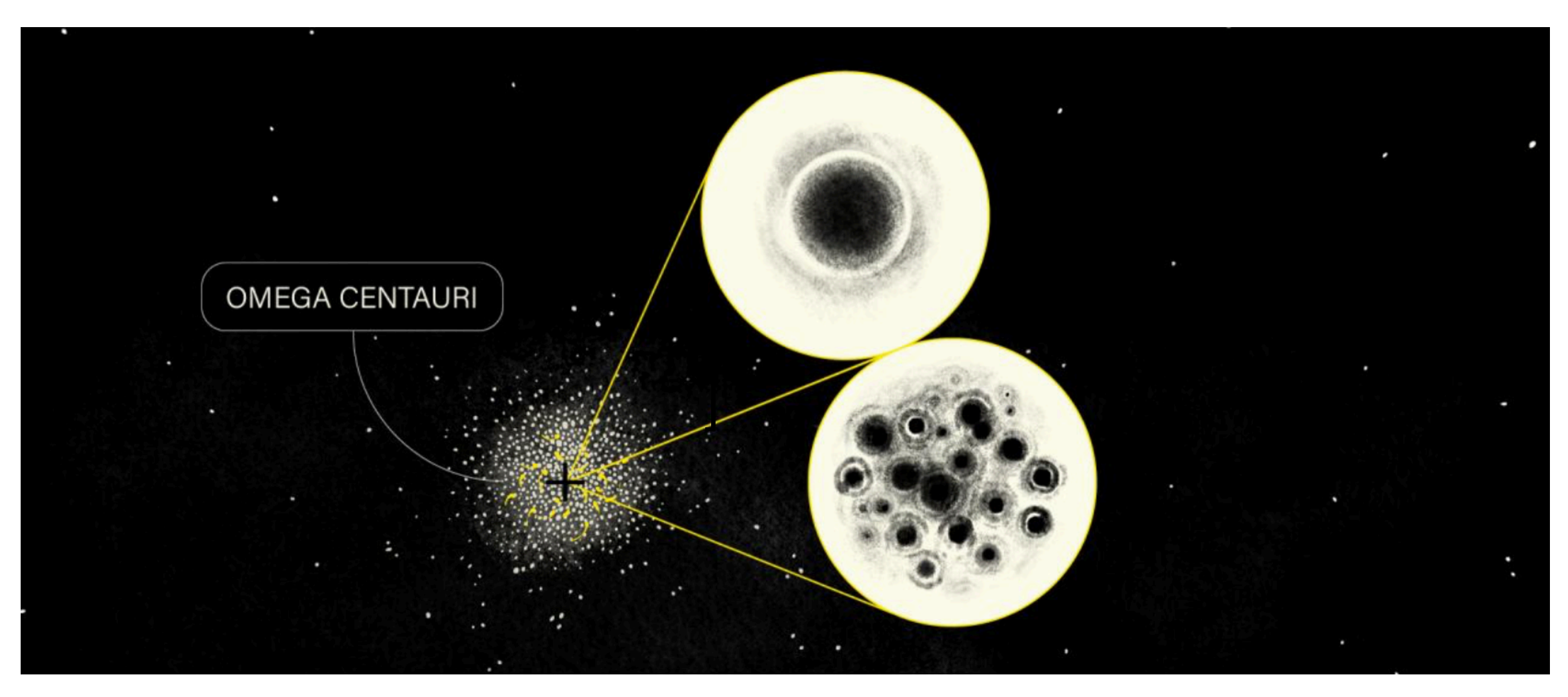








Is that the whole story?



https://www.iac.es/en/outreach/news/iac-researchers-find-stars-omega-centauri-move-under-action-cluster-black-holes

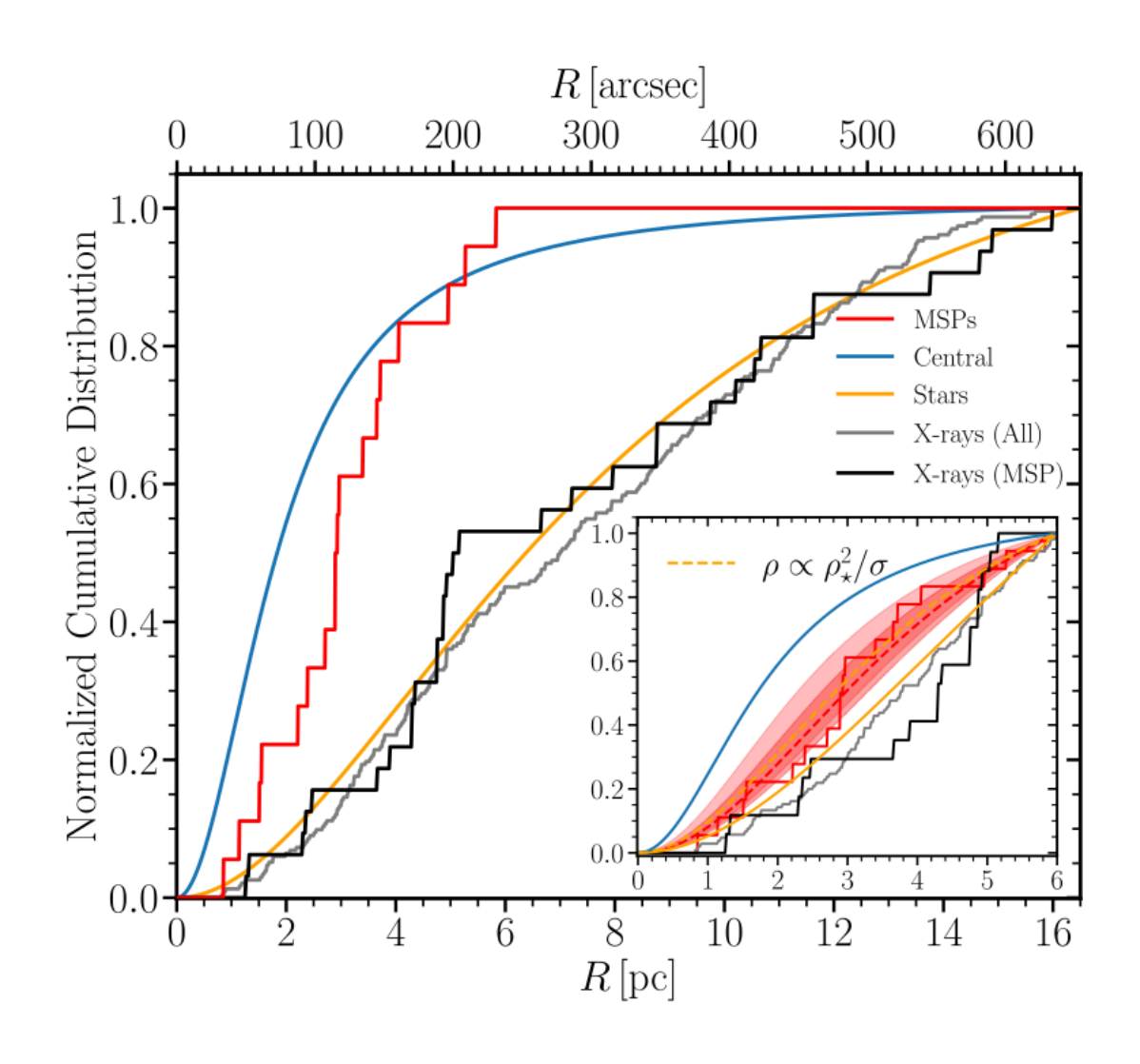






Two-component model with a significantly extended central mass distribution

Alongside the possible presence of dark matter, ω Cen is interesting as a possible location for the formation of black hole seeds via runaway stellar collisions (e.g. Portegies Zwart et al. 2004) or the formation and death of a supermassive star (e.g. Chon & Omukai 2020). Several authors (Noyola et al. 2008; Noyola et al. 2010; Jalali et al. 2012; Baumgardt 2017) found evidence of a $\sim 3 - 5 \times 10^4 \, \mathrm{M}_{\odot}$ intermediate-mass black hole (IMBH) at the center of ω Cen from the consideration of stellar kinematic data (using either Jeans models or N-body simulations). However, Van der Marel & Anderson (2010), via a Jeansbased analysis, derived a 3σ upper bound on the IMBH mass of 1.8×10^4 M_{\odot}, in tension with the previously cited masses. Baumgardt et al. (2019) also found no evidence of an IMBH by comparing N-body simulations to data for ω Cen (stellar velocity dispersion, surface brightness, and proper motion data), favoring instead a centrally concentrated cluster of stellar-mass black holes that accounts for 4.6% of the mass of ω Cen. Zocchi et al. (2017) and Zocchi et al. (2019) stress that the presence of an IMBH in ω Cen can be degenerate with orbital anisotropy and with the presence of a cluster of mass-segregated stellar-mass black holes. Evans et al. (2022) concluded that a core of stellar remnants can account for up to $\sim 5 \times 10^5 \ M_{\odot}$ of the inner dark mass derived in their analysis, with a dark matter also being a potential explanation. Therefore, the structure and composition of the mass content of ω Cen remains a subject of ongoing debate.



Bañares-Hernandez et al. 2024





